Waste and Biomass Valorization (2025) 16:6785–6792
https://doi.org/10.1007/s12649-025-03082-w

SHORT COMMUNICATION

Characterizing the Internal Structure of Biomass Pellets with Three-Dimensional Imaging

Jari Hyväluoma[1] · Riikka Keskinen[1] · Ari-Matti Seppänen[1] · Markus Hannula[2] · Kari Ylivainio[1]

Received: 23 October 2024 / Accepted: 21 April 2025 / Published online: 10 May 2025

Abstract

Pelleting is a common technique used to process loose biomass into a densified form. Pelleting packs the feedstock material tightly while forming a complex pore network between the solid constituents, which allows access of water and other substances to the interior parts of pellets. The characteristics of this pore system depend on the raw material and pelleting parameters. In pelleted recycled and organic fertilizers, the properties of the pore system partly determine the degradation of the pellets in soil and consequently the release of nutrients to plant available form. The fertilizer pellet structural properties have rarely been studied quantitatively at the pore level, whereby we conducted a three-dimensional imaging study using X-ray tomography to quantitatively analyse the pore characteristics of six pellet types, comprising three raw materials and two compression ratios. The image analysis revealed that both the raw material and compression ratio affected the internal pore structure of pellets. These findings suggest that the internal porous structure of fertilizer pellets can be tailored on length scales which affect the interaction of fertilizer with the surrounding soil and consequently affect the agronomic performance of the fertilizer.

Statement of Novelty

The loose and bulky structure of many recycled fertilizers complicates their exploitation. Therefore, densification of the raw materials by pelleting can increase the agronomic use of recycled fertilizers. Little is known about how the properties of raw material and processing parameters affect the pore system formed during pelleting. Previous studies have concentrated on energy pellets, whereas in the present work, the focus was on recycled fertilizers. Three-dimensional imaging with X-ray tomography was used to quantitatively analyse the pore structure within pellets produced from three different biomasses (sewage sludge, meat bone meal, straw). Our results showed that both the raw material and the compression ratio in pelleting can have notable effects on the internal pore structure of biomass pellets.

Keywords Pellet · Pore Structure · Organic Fertilizer · X-ray Tomography

Introduction

Recycling and transitioning from a linear to a circular economy have attracted interest throughout society including the agricultural sector, whereby various side streams and biomasses have been considered as fertilizers or soil conditioners for improving nutrient circularity in the food system [1, 2]. As the concentration of nutrients in recycled fertilizer products is typically lower than in mineral ones, the use of these products leads to increased demands and higher costs for transportation and storage [3]. Recycled fertilizers also often have loose and bulky structure complicating the handling and spreading.

The physical and agronomical attributes of recycled fertilizers can be processed to improve their storage, handling, and spreading properties and reduce the associated costs [4–6]. To create high-quality products and increase the use of recycled fertilizers, it is beneficial to increase their density and process them into compressed and granulated forms.

✉ Jari Hyväluoma
jari.hyvaluoma@luke.fi

[1] Natural Resources Institute Finland (Luke), Jokioinen, Finland

[2] Computational Biophysics and Imaging Group, Faculty of Medicine and Health Technology, Tampere University, Tampere, Finland

Pelleting is a common technique for densification of biomasses [7, 8]. In pelleting, biomasses derived from a range of organic sources [9], are compressed into cylindrical pellets with regular shape and size, which can resolve several drawbacks related to loose materials.

Pellets have varying internal structures depending on the feedstock type and properties, possible additional bulking agents, and processing parameters, which affect the mechanical properties of the pellets such as density, strength and durability [10]. In general, as compared to loose feedstock material, the breakdown and decomposition rate of pellets are slower. Regarding fertilizer pellets, the porous structure also affects the dissolution of the pellet and the pellet-soil-water interactions. Pelleting has been found to reduce phosphorus availability in biobased fertilizer pellets [11]. Larger pores allow water and microorganisms to easily enter the fertilizer pellet and enable nutrients to be easily mobilized over time thus making them available for plant uptake [12]. Thus, regulating the pore structure within fertilizer pellets offers one possibility of adjusting the release rate of the nutrients, which also provides the advantage of pelleted fertilizers over bulk form [13].

To better understand the functioning of fertilizer products, it would be beneficial to investigate the internal pore structure of the pellets, and how this structure is affected by feedstock or how it can be engineered by processing parameters. X-ray tomography provides a powerful tool to image the three-dimensional internal structure of porous materials at micrometre resolution [14]. X-ray tomography has been previously utilized in imaging various forms of energy pellets, including studying the correlation between the microscale properties of switchgrass pellets and the quality of the end product [15], characterization of pore structure of pyrolysed softwood pellets [16], development of cracks and cavities during combustion of poplar and wheat-straw pellets [17], and degradation of wood pellets and consequent crack formation during storage [18]. The internal structure of organic fertilizer pellets has been much less studied by direct three-dimensional imaging. The only study that the authors are aware of is the work of Valentinuzzi and coworkers [12], which considered digestate pellets from biogas production. Their study was limited to a small number (3) of samples and used commercial pellets whereby processing parameters were not reported. The imaged fertilizer pellets had complex internal pore networks which emphasizes the importance of additional studies on the internal structure of fertilizer pellets.

As the knowledge of the structure of pelleted organic fertilizers is still incomplete, the present work aimed at conducting a three-dimensional imaging study of pellets produced from three different biomasses. We considered two fertilizer products based on sewage sludge and bone meal. As a reference material, we considered barley straw. Each feedstock was pelleted using two compression ratios to consider the effect of varying process conditions. Our study hypothesis was that both the feedstock and processing have notable effects on the pellet pore structure. This study provides information about the possibility of influencing the pore structure within biomass pellets, which likely affects their functioning as fertilizers or soil amendments.

Materials and Methods

Pellets

Pelleting experiments were conducted with an Amandus Kahl 14–175 Laboratory Press, which operates with 175 mm flat dies and 3 kW power. Trial runs were carried out with three different materials (dried sewage sludge, meat bone meal and barley straw) and two different 4 mm diameter pellet dies with 4:1 (16 mm active pressing channel length) and 7.5:1 (30 mm active pressing channel length) compression ratios. The dimensions of the pellet dies were the following: diameter 175 mm, thickness 30 mm and taper angle 40°. A total of six pellet types were thus produced. During the operation, the temperature of the produced pellets was followed with an infrared thermometer and the temperature of the pellet die with the thermocouple of the pellet press. The pellet temperatures were 56 °C and 64 °C for sewage sludge (compressions 4:1 and 7.5:1, respectively), 30 °C and 50 °C for meat bone meal, and 36 °C and 73 °C for barley straw. The temperatures of pellet die were, in turn, 27 °C and 20 °C for sewage sludge (compressions 4:1 and 7.5:1, respectively), 19 °C and 28 °C for meat bone meal, and 21 °C and 31 °C for barley straw. The physicochemical properties of the used feedstock and produced pellets are given in Table 1. Regarding the particle size distribution of the feedstock, barley straw was milled through a 5 mm mesh prior to pelleting. The total concentrations of C, H, N and S were analysed through dry combustion with a CHN628 + 628 S Elemental Analyzer. The ash contents were determined at 550 °C usingTGA701 Thermogravimetric Analyzer. The pellet densities were determined by weighting sample pellets and measuring their diameter and length using a digital vernier calliper to calculate the pellet volume.

X-ray Tomography

The three-dimensional structural characterization of the pellets was conducted with X-ray microtomography. Four replicate samples were imaged from each six sample types. Pellets were scanned with a Zeiss Xradia MicroXCT-400

Table 1 Physicochemical properties of the used feedstock materials and produced pellets

	Sewage sludge	Meat bone meal	Barley straw
Ultimate analysis [%]			
C	34.92 ± 0.10	39.06 ± 0.20	43.28 ± 0.17
H	5.48 ± 0.06	5.98 ± 0.03	6.21 ± 0.03
N	4.95 ± 0.04	9.01 ± 0.06	1.74 ± 0.13
S	0.710 ± 0.002	0.431 ± 0.018	0.127 ± 0.011
Ash content [%]	31.9 ± 0.2	27.6 ± 0.2	9.1 ± 0.2
Particle size distribution [%]			
> 3.55 mm	23.4	3.6	nd*
1–3.55 mm	44.9	9.6	nd*
< 1 mm	31.7	86.8	nd*
Pellet density [g cm^{-3}]			
4:1	1.36 ± 0.03	0.97 ± 0.05	1.12 ± 0.13
7.5:1	1.33 ± 0.01	1.37 ± 0.04	1.25 ± 0.06

*nd = not determined

(Zeiss, Pleasanton, USA) device using the same imaging parameter values for all samples. Each scan consisted of 1601 2D projection images evenly distributed over a full 360° rotation. The exposure time was 5 s for each projection image. A 10× objective was used with a binning of 2, which resulted in a pixel size of 2.275 µm. The source voltage was 80 kV and the source current was 125 µA. LE2 filter was used in the imaging. The three-dimensional reconstructions were created of the projection images using the device manufacturer's Zeiss XMReconstructor software (Zeiss, Pleasanton, USA), which is based on the filtered back projection algorithm.

Image Processing and Analysis

The greyscale levels of the 16-bit images obtained from X-ray tomography were normalized and converted to 8-bit images using percentile stretching. The 1 and 99 percentiles of the greyscale values were set to 0 and 255, respectively, and the intermediate values were obtained with linear scaling. The greyscale images resulting from X-ray tomography were denoised with a three-dimensional variance-weighed mean filter with a radius of 2 voxels [19]. After denoising, images were segmented into pore and solid phases. A range of automatic segmentation algorithms available in the ImageJ software [20] were tested, but they did not result in satisfactory outcomes. Therefore, segmentation was done by manual thresholding where the threshold greyscale value was selected to give the best segmentation of pores and solids as compared to visual inspection. The same threshold value was applied for all bonemeal and sewage sludge pellet images. A different threshold value was used for the images of straw pellets, as these images had different greyscale levels than the other materials. The segmented images were further filtered with majority filter with a radius of 2 voxels and isolated solid objects smaller than 125 voxels were removed from the images.

The segmented images were analysed for porosity and pore size distribution. The pore size distributions of the imaged pellets were determined with mathematical morphology [21] by using a morphological opening algorithm with a sphere-shaped structuring element [22]. Morphological opening removes pores up to the size of the structuring element from the pore space, whereby pore size distribution is obtained by successive application of the opening process by structuring elements of increasing radius. Median pore diameters were determined from the pore size distribution.

Statistical Analysis

One-way analysis of variance (ANOVA) was carried out to compare the median pore sizes for different pellet raw materials and compressions. Multiple comparisons were conducted using Tukey's test. For pellet porosity, the assumption of homogeneity of variances was violated whereby the statistical comparisons for this quantity were carried out with Welch ANOVA and the multiple comparisons with the Games-Howell test. A significance level of $p < 0.05$ was used in statistical testing. The normality of the data was tested using Shapiro-Wilk's test, and homoscedasticity using Levene's test, both at a significance level of $p > 0.05$. Statistical analyses were performed with Python using the Stats module in the SciPy library [23] and the Pingouin package [24].

Results and Discussion

Visualizations of the internal structure of three selected pellets representing different raw materials and imaged by X-ray microtomography are shown in Fig. 1. Visualizations

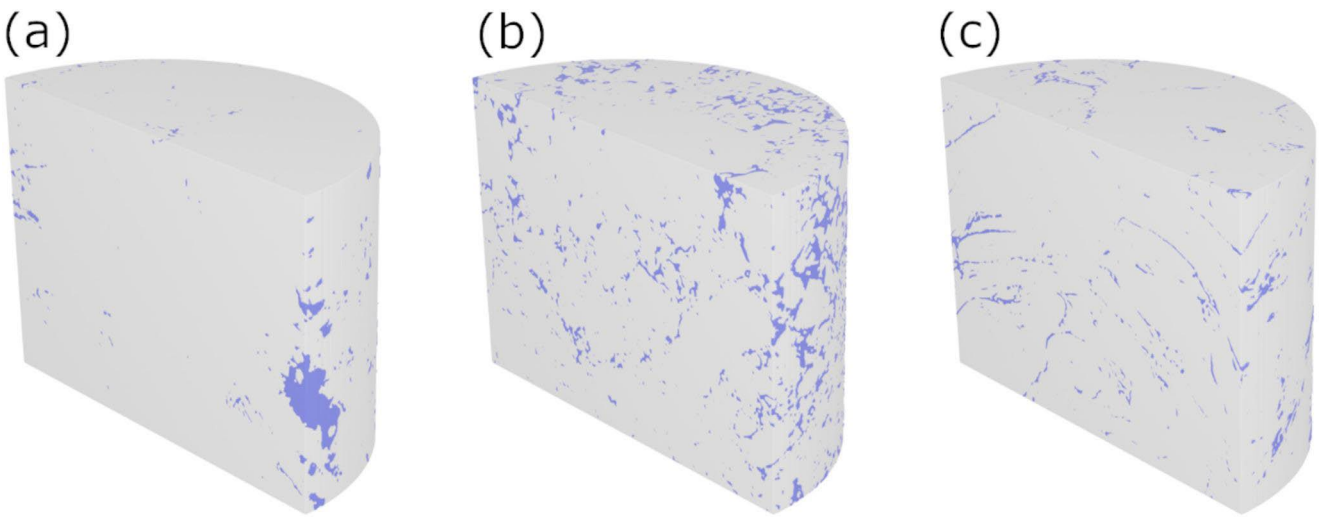

Fig. 1 Three-dimensional visualizations of three pellets made of differing raw materials: (**a**) Sewage sludge, (**b**) meat bone meal, and (**c**) barley straw. Pores and solid material are shown with blue and grey colour, respectively. The shown subvolumes have a diameter of 2.3 mm and a height of 1.5 mm. The compression ratio of all shown pellets was 4:1

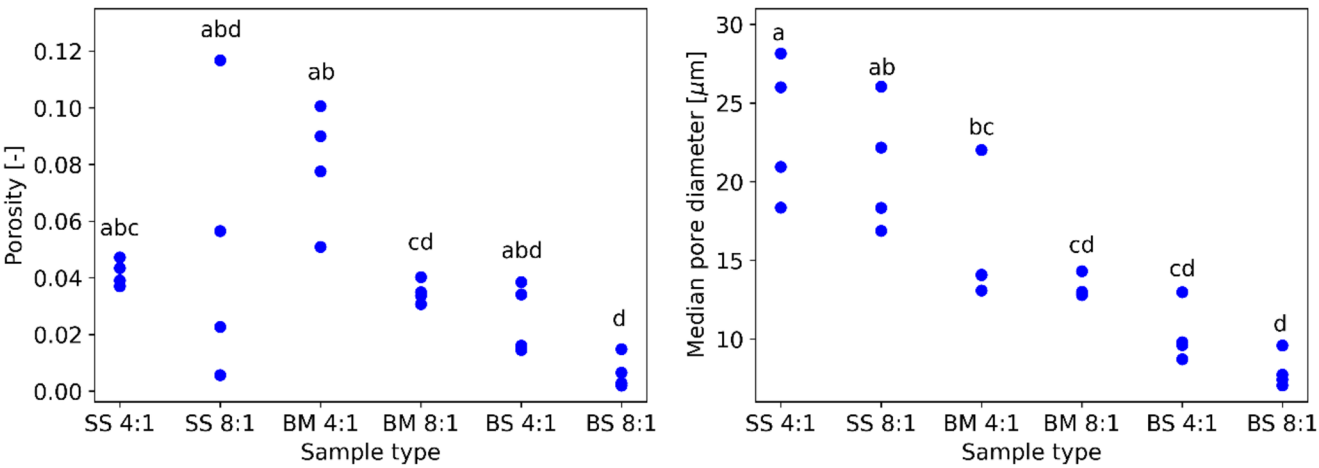

Fig. 2 Image analysis results for different pellet raw materials (SS = sewage sludge, BM = bone meal, BS = barley straw) and compression ratios (4:1, 7.5:1). (**a**) X-ray visible porosities of the pellets. (**b**) Median pore sizes determined from the computed pore size distributions. Separate data points are shown for replicate samples. Significant differences ($p < 0.05$) between pellet types are denoted by different letters

were done for segmented samples, and they thus show the organization of solids and voids in the pellets. Visual inspection indicates that pellets of different raw materials had contrasting internal pore structures. The sewage sludge pellet (Fig. 1a) had a lower number of pores and the porosity inside the pellet was heterogeneously distributed as compared with the meat bone meal pellet (Fig. 1b) which had a more homogeneous pore structure. The porosity of the straw pellet (Fig. 1c), in turn, was more anisotropic reflecting the characteristics of the raw material.

Image analysis revealed quantitative differences in the pore structure of different pellet types (Fig. 2). Statistical analysis showed that there are statistically significant differences between the means of porosity ($p < 0.01$) and median pore sizes ($p < 0.00001$) of the six different pellet types. Pairwise comparisons resulted in more evident differences in pore sizes compared to porosity. Considering porosity, for meat bone meal pellets there was a statistically significant difference between the two compression ratios, while for the two other materials such difference could not be proven. The porosity results were consistent with the measured pellet densities (Table 1). For sewage sludge, the measured pellet densities were almost the same for the two compression ratios and statistical analysis did not show a significant difference between them ($p = 0.99$). For meat bone meal, there was a clear and significant difference between the pellet densities ($p < 10^{-7}$) such that increased compression led to increased density consistently with the observed decrease

in the imaged porosity. For straw pellets, the density difference was merely marginally significant ($p=0.054$) and again the increased compression led to increased density. Median pore sizes confirmed that sewage sludge pellets had the largest pores, while the pore size of meat bone meal and straw pellets was smaller. These observations suggest that raw material properties affect the pelleting. For instance, a comparison of the particle size distributions of sewage sludge and meat bone meal (Table 1) shows that the latter material had smaller particle sizes which likely leads to smaller pore diameters.

While the results insinuate differences between raw materials and compression ratios, the small number of samples ($n=4$) and high variance within each sample group hinder drawing definite conclusions. The variance appeared to be largest for sewage sludge pellets that probably resulted from the iron present in the raw material, which as a high-density material lowered the quality of the images and therefore aggravated the identification of the pores.

To consider qualitative differences in the pellet pore system, Fig. 3 shows cross-sections of meat bone meal and straw pellets produced with different compressions (greyscale images show the X-ray attenuation coefficient inside the sample). These images show the differences between the two raw materials: meat bone meal pellet has granular structures and with higher compression, the inter-particle porosity seems to diminish. Straw pellet, in turn, has elongated pore shapes and the largest voids in the sample appear clearly less abundant with higher compression. Straw pellet with lower compression has also remnants of the cellular structures of the raw material, which are lesser in the pellet produced at higher compression.

These results show that there are differences in how different raw materials are packed during pelleting. Essentially, the pellet-forming abilities of different biomasses depend on their chemical and physical structure governing the formation and strength of inter-particle bonding [25]. Comparing the obtained porosity values with other research is hard as the previous imaging studies are limited to the work of Valentinuzzi et al. [12], who reported X-ray visible porosity values between 0.03 and 0.07 for digestate pellets imaged with a voxel size of 2.0 µm. These values are similar to our findings.

For different raw material types, variant pellet porosities have been observed with three-dimensional imaging. Note, however, that since compression ratio and pelleting parameters generally affect the pellet pore structure, comparison between pellets resulting from different sources is possible only on a qualitative level. Also, the imaging resolution affects the pore sizes that are visible in the images. The selected imaging resolution here was such that it allowed imaging of the whole pellet and was able to account for porosity responsible for water movement and storage in soil and microbial colonization, which are essential in fertilizer-soil-water interactions. The structure of pelleted and pyrolysed softwood was studied by Srocke and co-workers [16], who reported clearly higher porosity values (ca. 0.58). Their pellets retained the cellular structure of the raw material, which can explain the high porosity values. Pyrolysis has also been found to increase the porosity of organic materials [26]. Cutz et al. [18] studied pellets made of sawdust and in this case, the detected porosities varied around 0.05, which is comparable to the values observed in the present work. Edeh et al. [27] studied several pelleted biomasses including wheat straw and reported a porosity of 0.079. Their imaging resolution was higher with a voxel size of 0.87 µm which may explain somewhat larger porosities than what we found for barley straw pellets. Also, the typical pore size in the study of Edeh et al. [27] was similar to those observed here for barley straw pellets. However, we found clearly higher median pore sizes for sewage sludge and meat bone meal pellets which suggests that raw material impacts the pore sizes. Kim et al. [28] observed that small pore sizes delayed the uptake of water and release of nutrients from biochar-lignin pellets.

Cutz et al. [18] also found that storage led to an increase in the pellet porosity, which may reduce the pellet strength but also affect the transport properties of water and other substances. This finding suggests that changes in fertilizer pellet structure over time would be a topic for future research. X-ray tomography has also been applied to study the interaction of plant roots and mineral fertilizer granules [29]. A similar analysis could be interesting future research direction for pelleted organic fertilizers as the internal micrometre-range porosity can be expected to affect the root-fertilizer interaction.

Conclusions

Our results showed that both the raw material and the compression ratio in pelleting can have notable effects on the internal pore structure of biomass pellets and that there can be moderate variation in the pore properties also within the same pellet type. Here we considered pellets produced from three different raw materials by using two compression rates and the obtained results support our initial study hypothesis that both the feedstock and processing have notable effects on the pellet pore structure. Based on these findings, further studies with a broader selection of raw materials and processing parameters can be recommended. Understanding the factors that influence the characteristics and variation of the complex internal pore system of fertilizer pellets can help in predicting which pelleting parameters and feedstock

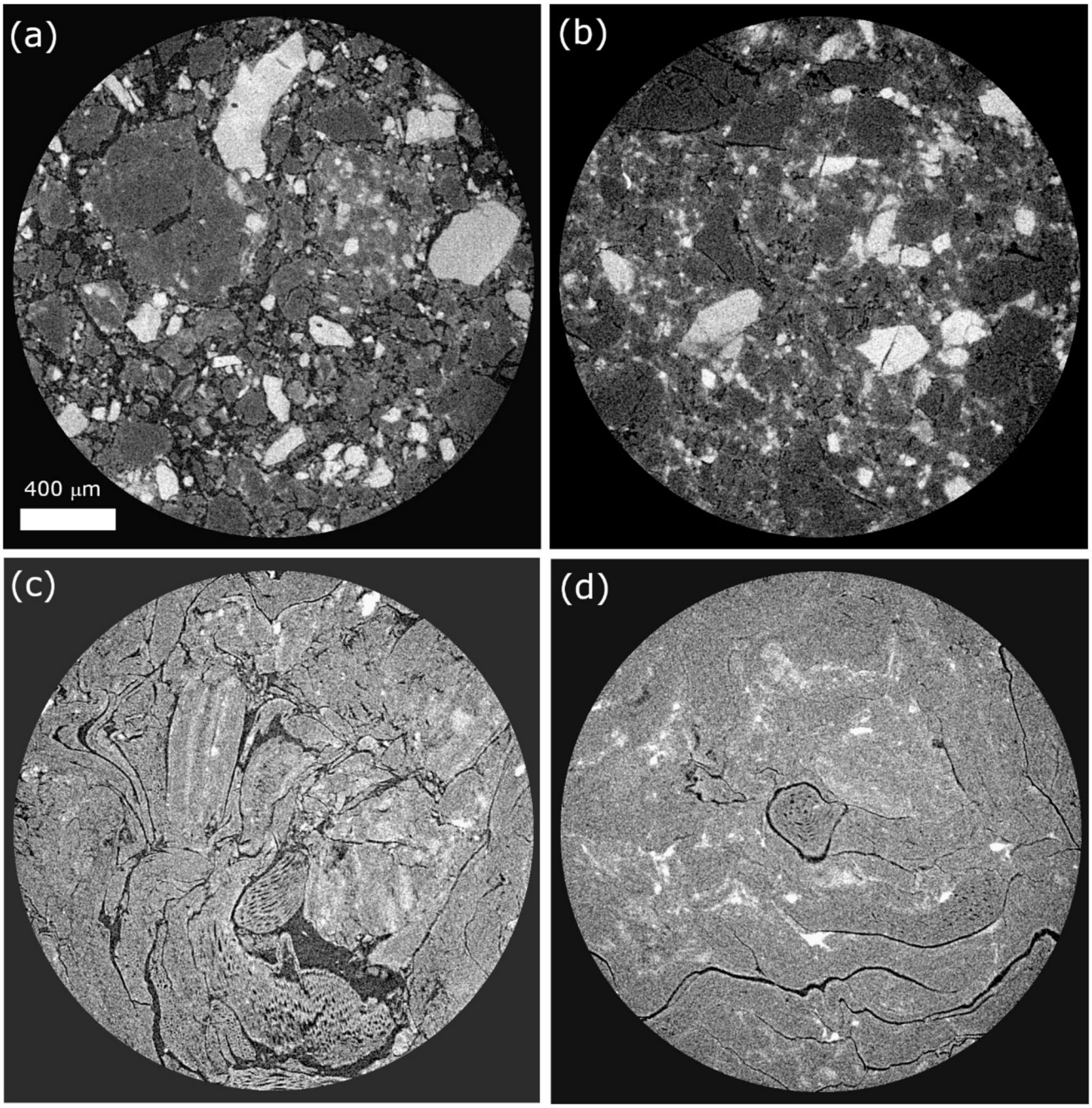

Fig. 3 Cross-sections of the grayscale images of selected pellets. A darker colour indicates lower material density (e.g. air) and higher densities are shown in a brighter colour. The diameter of each sample is ca. 2.1 mm. The shown pellets are meat bone meal pellets with compression ratios 4:1 (**a**) and 7.5:1 (**b**); barley straw pellets with compression ratios 4:1 (**c**) and 7.5:1 (**d**)

properties are most suitable for producing fertilizer products for different purposes from various feedstocks. The results suggest that it is possible to tailor the internal porosity of fertilizer pellets on length scales that are relevant for the functioning of the fertilizer in soil with impacts on for example the water transfer between the pellet and surrounding soil and microbial colonization. These can affect the release of nutrients for plants and affect the potential nutrient losses to the environment.

Acknowledgements This work was part of the "5R Refinery" co-innovation project funded by Business Finland (decision number 43794/31/2020).

Funding Open access funding provided by Natural Resources Institute Finland.
This work was part of the "5R Refinery" co-innovation project funded

by Business Finland (decision number 43794/31/2020).

Data Availability The data that support the findings of this study are available from the corresponding author upon reasonable request.

Declarations

Competing Interests The authors have no competing interests to declare that are relevant to the content of this article.

References

1. Harder, R., Giampietro, M., Smukler, S.: Towards a circular nutrient economy. A novel way to analyze the circularity of nutrient flows in food systems. Resour. Conserv. Recycl. **172**, 105693 (2021). https://doi.org/10.1016/j.resconrec.2021.105693
2. Koppelmäki, K., Helenius, J., Schulte, R.P.O.: Nested circularity in food systems: A nordic case study on connecting biomass, nutrient and energy flows from field scale to continent. Resour. Conserv. Recycl. **164**, 105218 (2021). https://doi.org/10.1016/j.resconrec.2020.105218
3. Ross, C.L., Mundschenk, E., Wilken, V., Sensel-Gunke, K., Ellmer, F.: Biowaste digestates: Influence of pelletization on nutrient release and early plant development of Oats. Waste Biomass Valoriz. **9**(3), 335–341 (2018). https://doi.org/10.1007/s12649-016-9794-8
4. Chew, K.W., Chia, S.R., Yap, Y.J., Ling, T.C., Tao, Y., Show, P.L.: Densification of food waste compost: Effects of moisture content and dairy powder waste additives on pellet quality. Process Saf. Environ. Prot. **116**, 780–786 (2018). https://doi.org/10.1016/j.psep.2018.03.016
5. Romano, E., Brambilla, M., Bisaglia, C., Pampuro, N., Pedretti, E.F., Cavallo, E.: Pelletization of composted swine manure solid fraction with different organic co-formulates: Effect of pellet physical properties on rotating spreader distribution patterns. Int. J. Recycling Org. Waste Agric. **3**(4), 101–111 (2014). https://doi.org/10.1007/s40093-014-0070-2
6. Sung-inthara, T., Juntahum, S., Senawong, K., Katekaew, S., Laloon, K.: Pelletization of soil amendment: Optimizing the production and quality of soil amendment pellets from compost with water and Biochar mixtures and their impact on soil properties. Environ. Technol. Innov. **33**, 103505 (2024). https://doi.org/10.1016/j.eti.2023.103505
7. Nielsen, S.K., Mandø, M., Rosenørn, A.B.: Review of die design and process parameters in the biomass pelleting process. Powder Technol. **364**, 971–985 (2020). https://doi.org/10.1016/j.powtec.2019.10.051
8. Gong, C., Meng, X., Thygesen, L.G., Sheng, K., Pu, Y., Wang, L., Ragauskas, A., Zhang, X., Thomsen, S.T.: The significance of biomass densification in biological-based biorefineries: A critical review. Renew. Sustain. Energy Rev. **183**, 113520 (2023). https://doi.org/10.1016/j.rser.2023.113520
9. Sarlaki, E., Kermani, A.M., Kianmehr, M.H., Vakilian, A., Hosseinzadeh-Bandbafha, K., Ma, H., Aghbashlo, N.L., Tabatabaei, M., M., Lam, S.S.: Improving sustainability and mitigating environmental impacts of agro-biowaste compost fertilizer by pelletizing-drying. Environ. Pollut. **285**, 117412 (2021). https://doi.org/10.1016/j.envpol.2021.117412
10. Kaliyan, N., Morey, V., R: Factors affecting strength and durability of densified biomass products. Biomass Bioenerg. **33**(3), 337–359 (2009). https://doi.org/10.1016/j.biombioe.2008.08.005
11. Sica, P., Müller-Stöver, D., Magid, J.: Formulating efficient P-rich biobased starter fertilizers: Effects of acidification and pelletizing on fertilizer properties. Circular Econ. 3, 100111 (2024). https://doi.org/10.1016/j.cec.2024.100111
12. Valentinuzzi, F., Cavani, L., Porfido, C., Terzano, R., Pii, Y., Cesco, S., Marzadori, C., Mimmo, T.: The fertilising potential of manure-based biogas fermentation residues: Pelleted vs. liquid digestate. Heliyon. **6**(2), e03325 (2020). https://doi.org/10.1016/j.heliyon.2020.e03325
13. Ball, B.C., McTaggart, I.P., Scott, A.: Mitigation of greenhouse gas emissions from soil under silage production by use of organic manures or slow-release fertilizer. Soil Use Manag. **20**(3), 287–295 (2004). https://doi.org/10.1079/sum2004257
14. Withers, P.J., Bouman, C., Carmignato, S., Cnudde, V., Grimaldi, D., Hagen, C.K., Maire, É., Manley, M., Plessis, A., Stock, S.R.: X-ray computed tomography. Nat. Reviews Methods Primers. **1**, 18 (2021). https://doi.org/10.1038/s43586-021-00015-4
15. Karamchandani, A., Yi, H., Puri, V.M.: MicroCT imaging to determine coordination number and contact area of biomass particles in densified assemblies. Powder Technol. **354**, 466–475 (2019). https://doi.org/10.1016/j.powtec.2019.06.002
16. Srocke, F., Han, L., Dutilleul, P., Xiao, X., Smith, D.L., Mašek, O.: Synchrotron X-ray microtomography and multifractal analysis for the characterization of pore structure and distribution in softwood pellet Biochar. Biochar. **3**(4), 671–686 (2021). https://doi.org/10.1007/s42773-021-00104-3
17. Strandberg, A., Thyrel, M., Skoglund, N., Lestander, T.A., Broström, M., Backman, R.: Biomass pellet combustion: Cavities and Ash formation characterized by synchrotron X-ray microtomography. Fuel Process. Technol. **176**, 211–220 (2018). https://doi.org/10.1016/j.fuproc.2018.03.023
18. Cutz, L., Tiringer, U., Gilvari, H., Schott, D., Mol, A., de Jong, W.: Microstructural degradation during the storage of biomass pellets. Commun. Mater. **2**, 2 (2021). https://doi.org/10.1038/s43246-020-00113-y
19. Gonzalez, R.C., Woods, R.E.: Digital Image Processing, 3rd edn. Pearson Education International (2008)
20. Schindelin, J., Arganda-Carreras, I., Frise, E., Kaynig, V., Longair, M., Pietzsch, T., Preibisch, S., Rueden, C., Saalfeld, S., Schmid, B., Tinevez, J.Y., White, D.J., Hartenstein, V., Eliceiri, K., Tomancak, P., Cardona, A.: Fiji: An open-source platform for biological-image analysis. Nat. Methods. **9**(7), 676–682 (2012). https://doi.org/10.1038/nmeth.2019
21. Horgan, G.W.: Mathematical morphology for analysing soil structure from images. Eur. J. Soil. Sci. **49**, 161–173 (1998). https://doi.org/10.1046/j.1365-2389.1998.00160.x
22. Hilpert, M., Glantz, R., Miller, C.T.: Calibration of a pore-network model by a pore-morphological analysis. Transp. Porous Media. **51**, 267–285 (2003). https://doi.org/10.1023/A:1022384431481
23. Virtanen, P., Gommers, R., Oliphant, T. E., Haberland, M., Reddy, T., Cournapeau,D., Burovski, E., Peterson, P., Weckesser, W., Bright, J., van der Walt, S. J., Brett,M., Wilson, J., Millman, K. J., Mayorov, N., Nelson, A. R. J., Jones, E., Kern, R.,Larson, E.,…

Vázquez-Baeza, Y. (2020). SciPy 1.0: fundamental algorithms for scientific computing in Python. Nature Methods, 17(3), 261–272. https://doi.org/10.1038/s41592-019-0686-2
24. Vallat, R.: Pingouin: Statistics in Python. J. Open. Source Softw. **3**(31), 1026 (2018). https://doi.org/10.21105/joss.01026
25. Anukam, A., Berghel, J., Henrikson, G., Frodeson, S., Ståhl, M.: A review of the mechanism of bonding in densified biomass pellets. Renew. Sustain. Energy Rev. **148**, 111249 (2021). https://doi.org/10.1016/j.rser.2021.111249
26. Turunen, M., Urbano-Tenorio, F., Rasa, K., Hyväluoma, J., Rytkönen, P., Kaseva, J., Beuker, E., Suhonen, H., Jyske, T.: How clonal differences and within-tree heterogeneity affect pore properties of hybrid Aspen wood and Biochar?? Biomass Convers. Biorefinery. **13**, 4061–4073 (2023). https://doi.org/10.1007/s13399-021-01464-3
27. Edeh, I.G., Masek, O., Fusseis, F.: 4D structural changes and pore network model of biomass during pyrolysis. Sci. Rep. **13**, 22863 (2023). https://doi.org/10.1038/s41598-023-49919-z
28. Kim, P., Hensley, D., Labbé, N.: Nutrient release from switchgrass-derived Biochar pellets embedded with fertilizers. Geoderma. **232–234**, 341–351 (2014). https://doi.org/10.1016/j.geoderma.2014.05.017
29. Ahmed, S., Klassen, T.N., Keyes, S., Daly, M., Jones, D.L., Mavrogordato, M., Sinclair, I., Roose, T.: Imaging the interaction of roots and phosphate fertiliser granules using 4D X-ray tomography. Plant. Soil. **401**(1–2), 125–134 (2016). https://doi.org/10.1007/s11104-015-2425-5